Revista de la Sociedad Geológica de España 29 (1)

ISSN (versión impresa): 0214-2708
ISSN (Internet): 2255-1379

MULTIFRACTAL CHARACTERISTICS OF BED THICKNESS IN THE LATE TURONIAN – EARLY CONIACIAN SEQUENCE (IBERIAN RANGES, SPAIN)

Características multifractales del espesor de estratos en la secuencia Turoniense superior –Coniaciense inferior (Cordillera Ibérica, España)

José F. García-Hidalgo[1], Javier Gil[1], Mónica Arias[2], Pablo Gumiel[2], Beatriz Carenas[3]

[1]*Grupo Ibercreta, UAH Research Team CCTE 2007/R23. Departamento de Geología, Geografía y Medio Ambiente. Universidad de Alcalá. 28871 Alcalá de Henares, Spain. jose.garciahidalgo@uah.es, javier.gil@uah.es.*
[2]*Departamento de Geología, Geografía y Medio Ambiente. Universidad de Alcalá. 28871 Alcalá de Henares, Spain. monica.ariasl@alu.uah.es. pablo.gumiel@uah.es*
[3]*Grupo Ibercreta, UAH Research Team CCTE 2007/R23. Departamento de Geología y Geoquímica. Universidad Autónoma de Madrid. Campus de Cantoblanco. 28049 Madrid, Spain. beatriz.carenas@uam.es*

Abstract*: A multifractal approach can help understand the controversy as to whether bed thickness obeys power law or log-normal distributions. In particular, late Turonian-early Coniacian bedding thickness distribution shows multiscaling properties related to structures that can be described as a collection of intertwined fractal subsets, which exhibit power-law scaling with a range of exponents and dimensions. The multifractal spectra discriminate between sections in different sedimentary environments (coastal, mixed and shallow marine). The correlation dimension (D_2) is equivalent to the thickness distribution dimension (D_t), and in the studied area has been used as a discrimination factor in the analysis of the distribution of sedimentary environments. Therefore, multifractal analysis can be considered as a useful tool to differentiate stratigraphic sequences, and can assist in the analysis of cyclicity and correlation at basin scale.*

Key-words: *Bed thickness, multifractals, multifractal spectrum, late Turonian-early Coniacian, Iberian Ranges.*

Resumen*: Una aproximación multifractal puede ayudar a entender la controversia sobre si el espesor de los estratos obedece a una distribución log-normal o fractal. En este sentido, la distribución de los espesores de estratos del Turoniense superior-Coniaciense inferior de la Cordillera Ibérica presenta propiedades multiescalares relacionadas con estructuras que pueden ser descritas como una colección de subconjuntos fractales entrelazados, que presentan escalas fractales en un amplio rango de exponentes y dimensiones. Los espectros multifractales pueden discriminar entre columnas localizadas en diferentes ambientes sedimentarios (costero, marino somero y la zona de indentación entre ambas). La dimensión de correlación (D_2) es equivalente a la dimensión fractal de distribución de espesores (D_t) y, en el área estudiada, se ha usado como un factor de discriminación en el análisis de la distribución de ambientes sedimentarios. En consecuencia, el análisis multifractal puede ser considerado como una herramienta útil para discriminar secuencias estratigráficas, y puede ayudar con el análisis de la ciclicidad y la correlación a escala de cuenca sedimentaria.*

Palabras clave: *Espesor de estratos, multifractales, espectros multifractales, Turoniense superior-Coniaciense inferior, Cordillera Ibérica.*

García-Hidalgo, J.F., Gil, J., Arias, M., Gumiel, P. y Carenas, B. (2016): Multifractal characteristics of bed thickness in the Late Turonian-Early Coniacian sequence (Iberian Ranges, Spain). *Revista de la Sociedad Geológica de España*, 29(1): 79-88.

The distribution and variation of bed thicknesses along stratigraphic sections have long attracted attention among researchers, mainly for stratigraphic analysis and modelling of sedimentary basins. From the seminal papers by Kolmogorov (1951), Pettijohn (1957), Mandelbrot and Wallis (1969) and Schwarzacher (1975), many workers have documented an approximately log-normal distribution for bed thicknesses (e.g., Pettijohn, 1957; Sadler, 1982; Drummond and Wilkinson, 1996; Talling, 2001, Sylvester, 2007); however, a power-law trend has also been proposed by other authors, based on outcrop (Carlson and Grotzinger, 2001; Longhitano and Nemec, 2005, Bailey and Smith, 2005) or well-logs and core analysis (Plotnick and Prestegaard, 1995; Gomez et al., 2002). It has even been proposed that parts of the stratigraphic record have exponential distributions and other parts do not (Burgess, 2008).

This debate can be represented by the papers of Talling (2001) and Carlson and Grotzinger (2001) on thickness distribution of turbidite beds; together with the paper by Sylvester (2007) on the same issue. Talling (2001) suggests that bed frequency distributions are the sum of a series of approximately log-normal distributions, which can produce a cumulative distribution with a segmented power-law trend. On the other hand, Carlson and Grotzinger (2001) suggest a separation between frequency distributions: While log-normal distributions correlate better with fan-lobe deposits, power-law distributions correlate better with interlobe deposits. They assume, however, that the primary signal is power-law although different sedimentary processes may have acted as a filter to modify this distribution systematically to a log-normal distribution. Finally, Sylvester (2007), using a more rigorous statistical analysis, suggests that the segmented power-law distributions are not a simple mixture of power-law distributions, but they can be considered a mixture of log-normal distributions, each with a different mean,

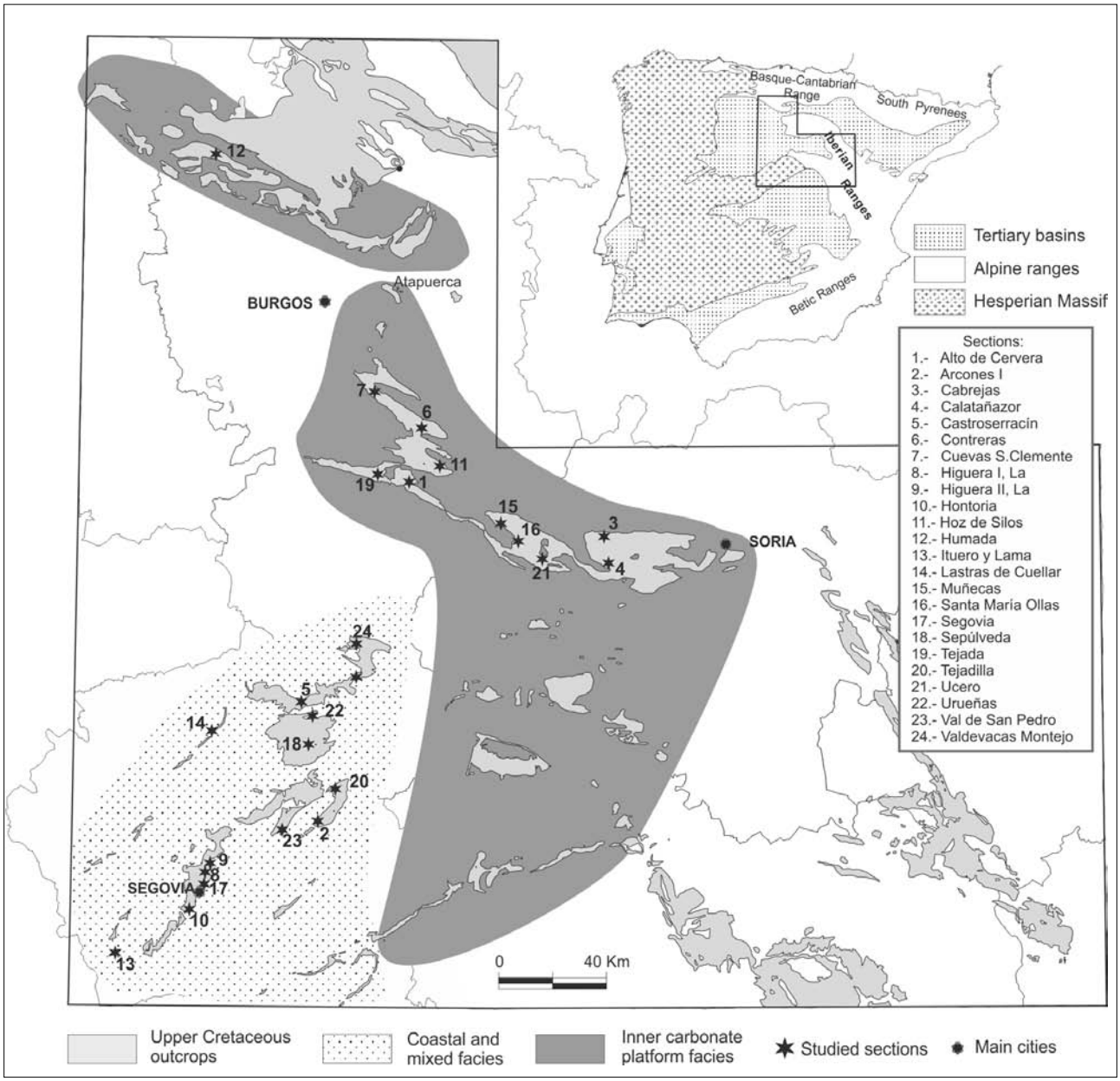

Fig. 1.- Location map of studied sections in the northern Central System and Iberian Ranges showing the Upper Cretaceous outcrops (light grey) and main depositional environments: coastal, mainly siliciclastic (dotted) and shallow marine environments, mainly carbonate (dark grey).

which mainly reflects differences in sedimentary processes within sedimentary basins.

These works suggest that there is a need for new quantitative studies and numerical modelling to explain how these distributions might have originated, to accurately understand the relations of these distributions to sedimentary environments, since it has been proposed that different depositional systems will have characteristic power-law patterns (Plotnick and Prestegaard, 1995). The objectives of this paper are focused on the question of whether thickness distributions of bedding have the statistical properties consistent with log-normal or power-law distributions or if they are systems with multifractal characteristics. These data, together with stratigraphic and sedimentary analysis, are tools to improve the knowledge of the temporary and spatial distribution of sedimentary patterns and processes at basin scale, which could be useful, for instance, in reservoir models, where bedding heterogeneity and spatial variation are of crucial importance, and for describing changes of sedimentary properties at basin scale, as an aid to understanding dynamics of depositional systems.

Geological setting

The late Cretaceous sedimentation in the Iberian Basin was controlled by the interplay of climate, tectonics and eustasy (Segura et al., 2002). During these times and specifically during the late Turonian–early Coniacian, Iberia had a subtropical location between 20º - 30º N (Dercourt et al., 2000), with a warm, humid climate. It was a time of relative tectonic quiescence in the Iberian Ranges and basin subsidence was relatively constant and mainly thermal (cooling) (Reicherter and Pletsch, 2000; Segura et al., 2001, 2002; Gil et al., 2001, 2004). On the other hand, a eustatic rise in sea level during the late Turonian, generated a narrow Atlantic seaway that flooded wide areas of the Iberian Basin, originating a carbonate ramp with a very low and regular depositional gradient with no significant sedimentary barriers or slope break, throughout the Iberian Basin (Muñecas Fm; Floquet et al., 1982; Floquet, 1991; Gil et al., 2004, 2006a and b); these shallow ramp sediments graded towards the Tethyan margin to littoral and carbonate coastal deposits (Alarcon Fm) (Gil et al., 2004), and towards the Iberian Massif margin first to mixed siliciclastic-carbonate facies (mainly composed of an alternation of dolostones and sands and clays, Caballar Fm, Floquet et al., 1982), and finally to coastal, siliciclastic deposits (Utrillas Fm; Gil et al., 2006a and b).

This study is mainly based on 24 stratigraphic sections of the late Turonian- early Coniacian 3rd-order sequence from the southern margin of the Basque-Cantabrian Ranges, the northern Iberian Ranges and the northern Central System (Fig. 1); the data series for each section includes part of the underlying and overlying sediments of this sequence due to two reasons: 1) we want tests of bed thickness distribution that are not restricted by major sequence boundaries, which could limit our interpretations; and 2) because extending the record, the amount of data is considerably increased for statistical analysis.

Studied sections (Fig. 1) were selected on the basis of accessibility and continuity of exposure. Individual beds were lithologically logged according to colour, grain size, sedimentary and biogenic structures, geometry and fossils. Detailed depositional analysis, sequence and parasequence stacking pattern and basin architecture have been described in detail by Gil et al. (2006a and b). The studied sequence comprises shallow marine carbonate deposits and their siliciclastic coastal margin sediments, with a lowstand shelf-margin wedge, a transgressive systems tract and a highstand systems tract (Gil et al., 2006a and b). The high-resolution stratigraphical architecture shows the superimposition of 4th to 6th order parasequences, which record short-term changes in the relative sea level (Gil et al., 2006a; 2009). Parasequence and cycle ranks here and herein reflect a standard concept used solely for description. A detailed cyclostratigraphic study and a bed to bed spectral analysis (Gil et al., 2009), suggest the existence of a complex cyclicity pattern made up of 4th-, 5th- and 6th-order parasequences superimposed within a long-term 3rd-order sequence. These parasequences show an astronomical tuning with the orbital periodicities in the Milankovitch frequency band, with long eccentricity cycles of 400 ka, short eccentricity cycles of 95 ka, and obliquity cycles of 39 and 50.6 ka, respectively (Gil et al., 2009). Thus, it is suggested (Gil et al., 2009) that in the late Turonian to early Coniacian of the Iberian Ranges, orbital forcing acted as a major factor that controlled climate and sea-level, which in turn influenced the depositional environments.

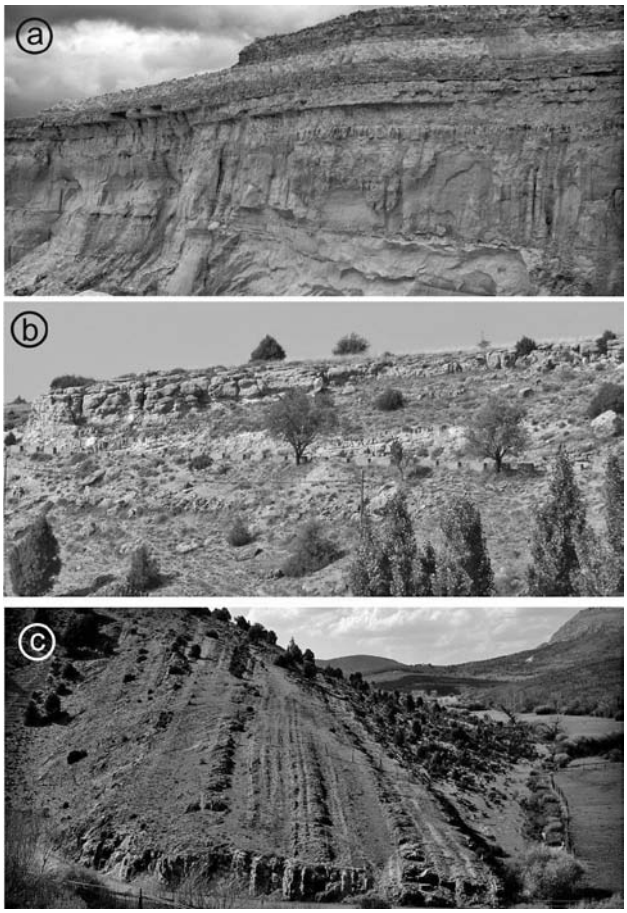

Fig. 2.- Field view of the selected sections discussed in text: a) Arcones section (2 in Fig. 1) with predominance of coastal facies, siliciclastic at the base and carbonate (dolomitic) at top (see Table 1); b) Valdevacas de Montejo section (24 in Fig. 1) with mixed facies; and c) Hoz de Silos section (11 in Fig. 1) with predominance of shallow marine carbonate facies. See also Fig. 3 for stratigraphic logs of these sections.

Studied sediments comprise shallow marine carbonate facies and their coastal fringe, composed mainly of siliciclastic facies (Table 1), with an area where both environments interdigitated (Gil et al., 2006a). Based on facies, study area has been divided into these three palaeogeographic areas (coastal, mixed and marine), and one section has been selected for each area to be shown in figures: Hoz de Silos in the carbonate shelf (11 in Fig. 1), Arcones in the coastal fringe (2 in Fig. 1) and Valdevacas (24 in Fig. 1) in the mixed area.

The sedimentary succession of the northern Iberian Ranges (Hoz de Silos section, Figs. 2 and 3) is entirely composed of carbonate shelf sediments, mainly medium-, to thick-bedded bioclastic limestones, for-algal limestones and marls (Table 1). The sedimentary succession at the eastern Central System shows a mixed siliciclastic-carbonate nature, with siliciclastic intercalations thinning upwards and the carbonate beds thickening upwards (Valdevacas section, Figs. 2 and 3). Here facies grade upwards from coastal sands, sandy dolostones and littoral limestones and marls, up to shallow marine bioclastic limestones and fossiliferous marls; stromatolitic beds and oolitic limestones are also common. The siliciclastic facies in coastal areas (Arcones section, Figs. 2 and 3), now located in the western Central System outcrops (Arcones to Ituero sections in Fig. 1), are composed of sands and sandstones, whitish caoliniferous silts and sands, and variegated clays grading upwards to dolostones (with common stromatolites) (Table 1). Since palaeogeographic changes for this sequence are subtle, any studied section mainly belongs to one of these three areas.

Data and methods

Cumulative frequency techniques (Drummond and Wilkinson, 1996; Burgess, 2008) for both log-normal and power-law have been applied to the study of thickness distribution for these sections. Each data set consists of a measured field section of continuously exposed beds (only locally are some minor sandy and marly beds semicovered) (Fig. 1, Table 2). Thicknesses were measured normally for the bedding, and laminations and cross-bedding laminations have not been considered as bedding. Section thicknesses range from 25.45 m up to 131.3 m; total thickness of the studied sections is 1550.55 m (Table 2). The number of beds (n) per section is between 36 and 216, which is suitable for statistical analysis (Milenkovíc, 1989), with a total of 1883 beds. Mean bed thickness is 0.81 m and the modal class is 0.2 m (Table 2).

The goodness-of-fit results for log-normal (Table 2; Fig. 4A, D, G), cumulative probability plots (Fig. 4B, E, H) and log-log plots (power-law) distributions (Fig. 4C, F, I) fit the data

Environments	Facies	Lithology	Fossils and traces
Shallow carbonate shelf	Fossiliferous marls	Thick-bedded, homogeneous, grey marls.	Echinoderms, bivalves, gastropods, oysters.
	For-algal limestones	Thick- to very thick-bedded (up to 1 m thick), massive, wackestone to packstone.	Green algae, benthic foraminifera, discorbids bivalves, bryozoans, echinoderms ammonites. Burrowing rare to common
	Bioclastic limestones	Medium- to thick-bedded, bioclastic wackestone to packstone	Gastropods, benthic foraminifera, echinoderms, bivalve fragments.
	Oolitic limestones	Medium-bedded, oolitic and bioclastic packstone to grainstone	Benthic foraminifera, echinoderm fragments, gastropods.
	Stromatolitic limestones	Thin-bedded, hemispheroid, stromatolitic	Stromatolites. Rare annelid colonies.
	Burrowed clays and marls	Nodular, yellow and grey clays and marls.	Rare bivalves, gastropods, oysters. Burrowing is common
Coastal	White sands	Thick- to very thick-bedded sands and sandstones (and gravels). Erosive bases, cross bedding, HCS, mud drapes, wavy bedding, ferruginous surfaces.	None
	Silts and clays	Thin- to thick-bedded caoliniferous silts, green to red clays. Massive, rare lenticular bedding, ferruginous surfaces, mud cracks.	Rhizolites (root traces)
	Sandy dolostones	Medium-bedded, red, sandy dolostones. Ripples lamination.	None
	Limestones and calcareous marls	Thin-bedded laminated wackestone to packstone. Wavy bedding, flaser and lenticular bedding.	Bivalve fragments
	Dolostones	Thin- to medium-bedded, laminated, massive or brecciated, yellow and brown dolostones. Microkarst, palaeosols.	Stromatolites, undetermined bioclasts. Burrowing rare to absent

Table 1.- Environments and facies of the late Turonian-early Coniacian sequence; two main environments can be distinguished: Shallow carbonate shelf, and coastal , mainly composed of siliciclastic facies, but also carbonate ones. There is also a zone where both environments interdigitated in the sequence (based and modified from Gil et al., 2006a, 2006b).

sets using the coefficient of determination R^2. The Kolmogorov-Smirnov, Chi-square test and P-values (Table 2) suggest that most sections have a good fit with a log-normal distribution (Pettijohn, 1957; Schwarzacher, 1975; Talling, 2001; Sylvester, 2007). There are sections, however, with very low p-values, suggesting that these sections also have characteristics of exponential (power-law) distributions.

However, there is also a defined straight part of the log-log plots with a negative slope, and two tails at the lower and upper ends (Fig. 4C, F and I), with a minimum mean thickness of 0.34 m, and a maximum mean thickness of 3.47 m (Table 2). Within these ranges, the R^2 data show values greater than 0.95 for all the 24 studied sections, with up to 10 sections in the range of 0.99 (Table 2). This supports the idea that thickness shows a power-law distribution in that range, with D_t values from 0.78 to 1.03 in the slope of the linear section (Table 2, Fig. 4C, F and I).

The fact that these distributions show both log-normal and power-law components suggests that they probably represent multifractal systems.

Multifractal approach to late Turonian bedding thickness distribution

In many natural records a single scaling exponent is not enough for a full description of the correlation structure of the data set, but rather an infinite number of exponents is needed (Feder, 1988, Turcotte, 1992). This kind of data is usually referred to as "multifractal", to distinguish it from "monofractal" long-term correlated data characterized by a single scaling exponent. This happens, for example, when values of different magnitudes follow different scaling laws (Ludescher et al., 2011).

Multifractal analysis has been applied to many natural complex systems, such as geochemistry and mineral deposits geology (i.e. Agterberg, 2007; Gumiel et al., 2010; Arias et al., 2011), and can also be related to specific probability distributions, most commonly the lognormal that is widely applicable to bedding distributions (Talling, 2001; Sylvester, 2007).

In a multifractal, spatial variations in the value of a property are assessed by a multifractal measure. If the measure

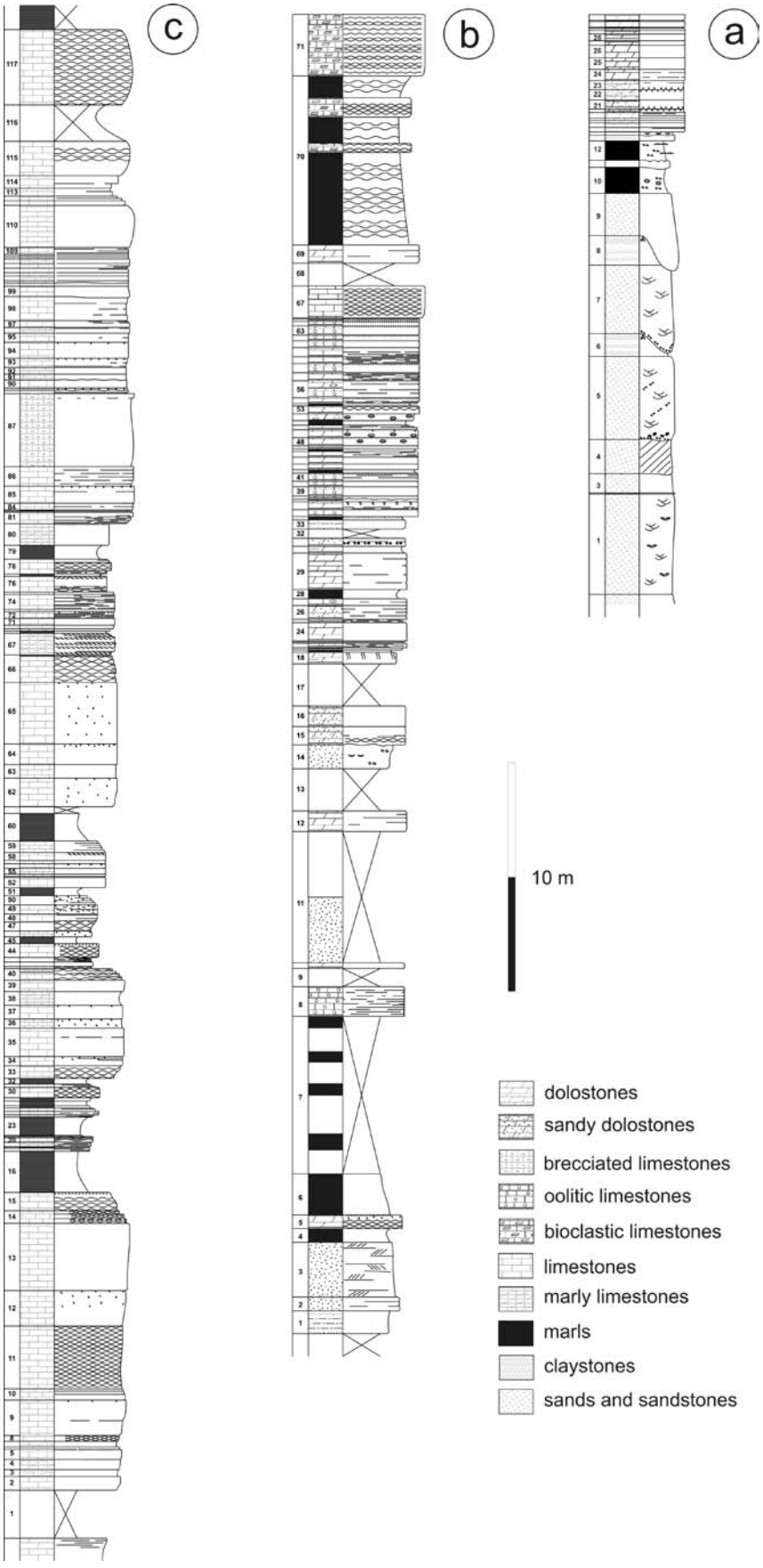

Fig. 3.- Stratigraphic logs of selected sections in studied area; a) Arcones section (2 in Fig. 1); b) Valdevacas de Montejo section (24 in Fig. 1); and c) Hoz de Silos section (11 in Fig. 1). See Fig. 2 for a field view of these sections.

Stratigraphic sections	Total thickness	Number of beds	Thinnest bed	Thickest bed	Corrected Dt	R2 corrected	Kolmogorov-Smirnov test	Chi-square test	P-value	Lower thickness*	Higher thickness*	R2 *
1, Alto de Cervera	77,90	86	0,05	8,5	0,78	0,91	0,0944	20,0973	0,0053	0,30	8,00	0,99
2, Arcones	26,05	34	0,05	4,4	0,61	0,93	0,0910	11,5642	0,1158	0,20	3,50	0,99
3, Cabrejas	81,45	117	0,05	6	0,74	0,82	0,0616	13,1763	0,2819	0,35	1,65	0,98
4, Calatañazor	66,75	67	0,05	10	0,87	0,87	0,0942	24,5840	0,0018	0,30	2,00	0,99
5, Castroserracín	109,25	119	0,05	7,9	0,82	0,93	0,1353	66,8593	0,0000	0,25	3,00	0,99
6, Contreras	69,35	117	0,05	4,6	0,86	0,90	0,1029	34,3559	0,0004	0,45	2,90	0,99
7, Cuevas de San Clemente	46,15	69	0,05	6,5	0,80	0,88	0,0997	12,9464	0,3729	0,25	6,50	0,98
8, Higuera I, La	27,60	62	0,05	3,2	0,68	0,90	0,1091	26,7047	0,0312	0,15	3,20	0,97
9, Higuera II, La	53,60	36	0,10	7,6	0,67	0,91	0,0893	23,4775	0,0529	0,35	7,00	0,97
10, Hontoria	25,45	36	0,05	2,45	0,60	0,81	0,1076	12,6705	0,3154	0,35	2,40	0,96
11, Hoz de Silos	64,05	116	0,05	3,3	0,83	0,90	0,0627	35,5510	0,0021	0,35	2,95	0,99
12, Humada	114,35	88	0,10	7,3	0,79	0,87	0,0620	15,2438	0,3617	0,55	2,10	0,98
13, Ituero y Lama	53,45	41	0,05	6,4	0,61	0,88	0,0851	11,1238	0,5183	0,30	2,40	0,98
14, Lastras de Cuellar	131,30	77	0,05	10,4	0,64	0,87	0,0597	25,0149	0,0029	0,50	5,50	0,99
15, Muñecas	60,45	139	0,05	2,9	1,03	0,82	0,0952	66,3775	0,0000	0,35	2,90	0,98
16, Santa María de las Ollas	61,30	78	0,10	12	0,98	0,89	0,0951	25,8428	0,0397	0,35	3,40	0,96
17, Segovia	51,65	68	0,05	4,5	0,68	0,87	0,1164	15,4816	0,0303	0,50	1,45	0,98
18, Sepúlveda	92,20	110	0,05	10	0,79	0,87	0,0982	17,4361	0,0258	0,50	1,75	0,98
19, Tejada	59,80	82	0,05	6,2	0,75	0,89	0,0749	45,4740	0,0000	0,45	2,10	0,99
20, Tejadilla	31,60	55	0,05	3,2	0,68	0,92	0,0887	89,7766	0,0000	0,40	0,80	0,97
21, Ucero	73,25	108	0,05	7,25	0,84	0,86	0,0817	30,6735	0,0037	0,35	7,25	0,98
22, Urueñas	43,95	52	0,05	6,4	0,77	0,91	0,1544	20,6784	0,0553	0,15	1,60	0,98
23, Val de San Pedro	72,15	55	0,05	7,75	0,47	0,93	0,0804	90,8502	0,0000	0,35	2,00	0,99
24, Valdevacas de Montejo	57,50	71	0,05	7,3	0,75	0,93	0,1430	40,2365	0,0002	0,20	6,90	0,99
Total and mean data	**1550,55**	**1883**				**0,89**				**0,34**	**3,47**	**0,98**

Table. 2.- Stratigraphic and statistical data of the stratigraphic studied sections. Main statistical data are for log-normal distribution. (*) Thicknesses in these ranges follow an exponential distribution (power-law).

shows self-similarity, it can be described as a multifractal (Evertsz and Mandelbrot, 1992). These authors present the partition function $\chi_q(\varepsilon)$ for each box size and a range of real numbers q:

$$(1) \qquad \chi_q(\varepsilon) = \sum_{i=1}^{N(\varepsilon)} \mu_i^q(\varepsilon) \qquad , \infty - \leq q \leq +\infty$$

The partition function is then plotted against the box size, and if the resulting graph produces a series of straight lines, the method can proceed to calculate the *mass exponent* $\tau(q)$, which is the slope of $\chi_q(\varepsilon)$ vs. ε in a log-log plot (equation 2).

$$(2) \qquad \chi_q(\varepsilon) \approx \varepsilon^{\tau(q)}$$

In general, two functions are used to represent the multifractality of a measure: the *multifractal spectrum* $f(\alpha)$ and the *generalized dimension* Dq (*Dq spectrum*).The $f(\alpha)$ represents the fractal dimension of the subsets with the same singularity index α. The singularity (α) quantifies the local degree of regularity of the distribution of a given set of objects. In this paper, α was calculated from equation (3) (Agterberg et al., 1996b) using a central finite difference method.

$$(3) \qquad \alpha = \frac{d\tau_q}{dq}$$

The $f(\alpha)$ curve is a convex function, specified by (Agterberg et al., 1996b):

$$(4) \qquad f(\alpha) = q(\alpha) - \tau(q)$$

If the plot $f(\alpha)$ vs. α is parabolic, and satisfies the conditions outlined by Evertsz and Mandelbrot (1992), the distribution is a continuous multifractal. It can be shown that α and $f(\alpha)$ are the Legendre transform variables of q and $(q-1)\,D_q$ (Cheng, 1994).

The *generalized dimension* D_q can be obtained from the relationship:

$$(5) \qquad D_q = \frac{1}{q-1}\,[q\alpha(q) - f(\alpha(q))] \qquad \text{, and} \quad \tau = (q-1)\,Dq$$

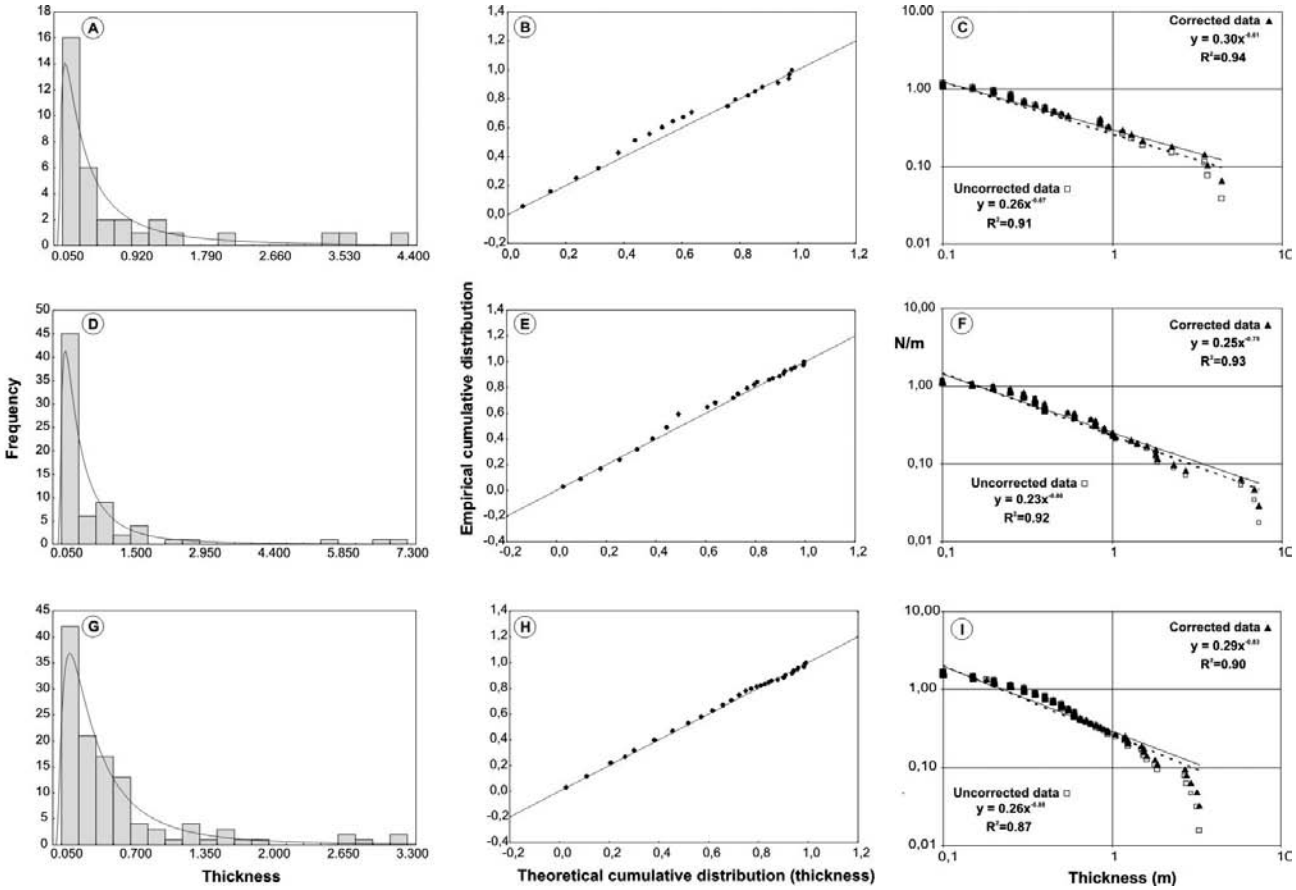

Fig. 4.- Frequency histograms (A, D and G) with the best fit to log-normal distributions. Cumulative probability plots of the thickness (B, E and H). Log-log plot of number of beds, N, with thickness higher than m (N/m) versus thickness (m) showing total data and the best fit to the power-law portion of the plot (C, F and I). Roll-off corrections (Pickering et al., 1995) to D_t plots have been considered (Table 2). To correct left and right hand truncations (LHT and RHT; Pickering et al., 1995), data that show LHT are excluded from the analysis. The correction method developed by Pickering et al (1995), which estimates the number of large size beds needed to correct the right hand curve of the plot to a straight line, was applied to correct any RHT (corrected data, Table 2). Arcones section (A, B and C); Valdevacas de Montejo section (D, E and F); Hoz de Silos section (G, H and I).

The two spectra *f(α)* and D_q describe the same aspects of any multifractal. They are equivalent and can be transformed to each other (Feder, 1988). A multifractal describes a non-random measure that is true for all $-\infty \leq q \leq +\infty$. For $q=0$, D_q represents the box-counting or *capacity dimension* (D_0) of the support of the measure. *If* $q=1$, then $\chi_\varepsilon(1)=1$, $\tau(1)=0$, *and* $f(\alpha(1))=\alpha(1)$, $\alpha(1)$ being the *information dimension* (D_1) which reflects the size of the set on which the measure μ is concentrated. D_2 is the *correlation dimension* and $q>2$ dimensions are usually referred to as the generalized dimension. For a homogenous fractal, $D_0=D_1=D_2$, but for multifractals $D_0>D_1>D_2$. Greater variation of D_q, with respect to q, implies a higher degree of heterogeneity of the measure. Therefore, *f(α)* and D_q can be used to compare the degree of clustering and heterogeneity of different distributions (Panahi and Cheng, 2004).

The existence of multifractals usually implies an underlying multiplicative cascade process, while additive processes tend to produce simple fractals or "monofractals" (Grassberger and Procaccia, 1983; Loehle and Li, 1996). Thus, in many nonlinear systems, a single value of the fractal dimension may not be enough to characterize the fractal properties of that system.

Bedding thickness distribution in the studied stratigraphic sections follows Brownian patterns, increasing cyclicity from the coastal (Arcones) to the carbonate sections (Hoz de Silos) (Fig. 5A to C).

In the multifractal analysis carried out we found that the multifractal spectra *f(α)* are the functions that best discriminate the bedding thickness distribution in the studied sections. Based on the obtained multifractal spectra three distinct groups, whose main representatives are the above mentioned sections, can be distinguished: Hoz de Silos, Arcones and Valdevacas representing the end-members of all studied sections (Fig. 5D). The spectra are generally symmetrical in shape (Fig. 5D) but their amplitude *(Δα)* and the values of *f(α)* are good discriminates of the considered sections, reflecting differences in the degree of homogeneity and consequently in the fractal dimensions.

The Hoz de Silos section shows the lower amplitude value ($\Delta\alpha = 0.412$) (Table 3, Fig 5D) reflecting the lower degree of multifractality of the studied sections, which agree with higher stratigraphical homogeneity (carbonate shelf). The Arcones shows an intermediate amplitude value ($\Delta\alpha = 0.784$) which corresponds to the coastal fringe. By contrast, the Valdevacas section shows the highest amplitude value ($\Delta\alpha = 1.123$), reflecting the highest degree of heterogeneity and multifractality of the sections that corresponds to the mixed area (Fig 5D). This can be related to the mixture of sedimentary processes that took

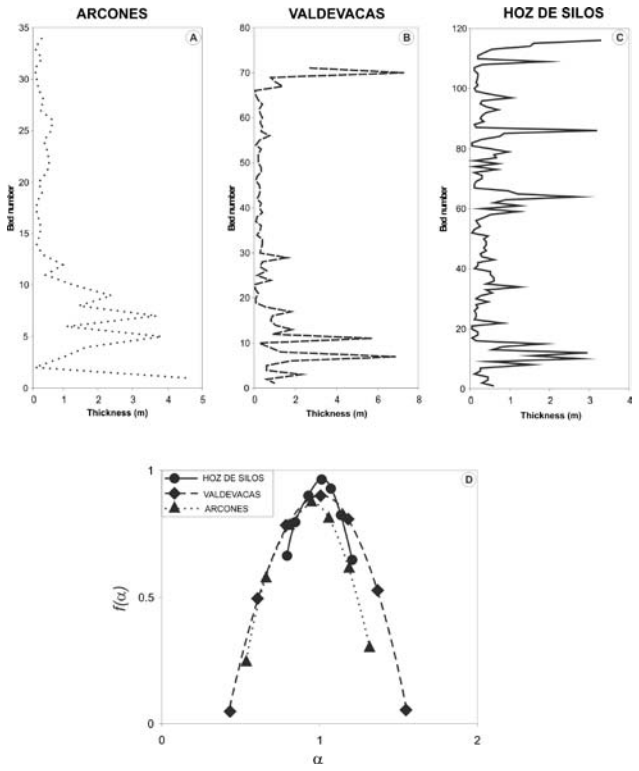

Fig. 5.- Thickness vs. bed number plots in the Arcones (A) Valdevacas (B) and Hoz de Silos (C) sections. These plots show Brownian patterns increasing the frequency and cyclicity from Arcones to Hoz de Silos. Multifractal spectra *f(α)* vs. α plot (D) showing clear differences in shape and amplitude between the three sections.

place in this area, in relation to the coastal and shallow marine environments interdigitation.

However, Hoz de Silos and Arcones sections show a more homogeneous behaviour within their sedimentary environments (either marine or coastal respectively). The result is the decrease of the multifractality degree, probably due to the presence of superimposition of periodicities in the sedimentary record or intermittency in the sedimentary processes. The first is the case of Hoz de Silos, where different cycle periodicities are clearly shown in spectral studies, showing an astronomical control on sedimentation, with several Milankovitch cycles superimposed (Gil et al., 2009). The second is the case of Arcones, where the presence of abundant scour surfaces and cross stratification indicates that deposition occurred in an environment characterized by the presence of shifting channels (Gil et al., 2006a).

Implications for sedimentary environment recognition

Fractal and multifractal analysis can be a useful tool for discrimination of sedimentary environments (Fig. 6). In particular, the Hurst exponent has been previously mentioned to distinguish between proximal and distal lobe settings in turbiditic environments (Felleti and Bersezio, 2010). The multifractal analysis shows that the correlation dimension (D_2) of these multifractal spectra is very close to the thickness distribution dimension (D_t). For this reason the latter has been used in the generation of maps of D_t distribution (Fig. 6), which can be compared with the distribution of sedimentary environments (Gil et al., 2006a) (Fig. 6b). Our data show that the different palaeogeographical areas can be clearly distinguished on the basis of (D_t) of the studied sections. Therefore, those sections composed mainly of coastal sediments (Arcones; 2 in Fig. 6a) have the smaller power-law dimensions, ranging from 0.47 to 0.68 (mean $D_t \approx 0.63$) (sector A in Fig. 6b). Sections where coastal and carbonate environments interdigitated (Valdevacas; 24 in Fig. 6a) have higher dimensions ranging from 0.74 to 0.79 (mean $D_t \approx 0.76$) (sector B in Fig. 6b). Finally, the marine carbonate sections (Hoz de Silos; 11 in Fig. 6a) have the highest values ranging from 0.80 to 1.03 (mean $D_t \approx 0.89$) (sector C in Fig. 6b).

Two sections, however, show some differences from this pattern: Cabrejas (3 in Fig. 6a), where a notable increase in the thickness of the basal part of the section is related to a tectonic event of the San Leandro Fault (Gil et al., 2006b); and Humada (12 in Fig. 6a), where shallow carbonate sediments alternate with deeper marls. The presence of anomalous tectonic activity acting during part of the sequence (Gil et al., 2006b) changes the number and thickness of beds in relation to other sections unaffected by tectonics, explaining this difference. On the other hand, the Humada section shows the transition to deeper environments where marl sedimentation was common (Gil et al., 2006a and b). The presence of these deep marls reduces the D_t dimension of the section and mimic values in the B area where off-shore clays were common (Gil et al., 2006a and b).

Finally, multifractal spectra help to discriminate the different palaeogeographic areas and these functions could therefore be considered as a new tool in the sedimentological analysis of stratigraphic sequences.

Conclusions

The main conclusions derived from the study carried out are summarized as follows:

1) Bed thicknesses of the studied stratigraphic sections show a fractal component in the intervals described in Table 2 (0.35-3.5 m).
2) All sections show a general multifractal behaviour which has been clearly shown by the obtained multifractal spectra *f(α)*. Based on these functions we can distinguish between three

	Dimensions			*α*	*f(α)*	*Δα*
Arcones	D_0	=	0.872	0.95	0.872	**0.784**
	D_1	=	0.806	0.809	0.779	
	D_2	=	0.746	0.661	0.576	
Valdevacas	D_0	=	0.9	1.008	0.9	**1.123**
	D1	=	0.81	0.8075	0.7775	
	D_2	=	0.715	0.605	0.495	
Hoz de Silos	D_0	=	0.963	1.013	0.963	**0.412**
	D1	=	0.927	0.928	0.898	
	D_2	=	0.893	0.845	0.797	

Table 3.- Values of the fractal dimensions; capacity dimension *(D_0)*, information dimension *(D_1)*, correlation dimension *(D_2)*, singularity *(α)*, *f(α)* values, and amplitude *(Δα)* of the Arcones, Valdevacas and Hoz de Silos sections.

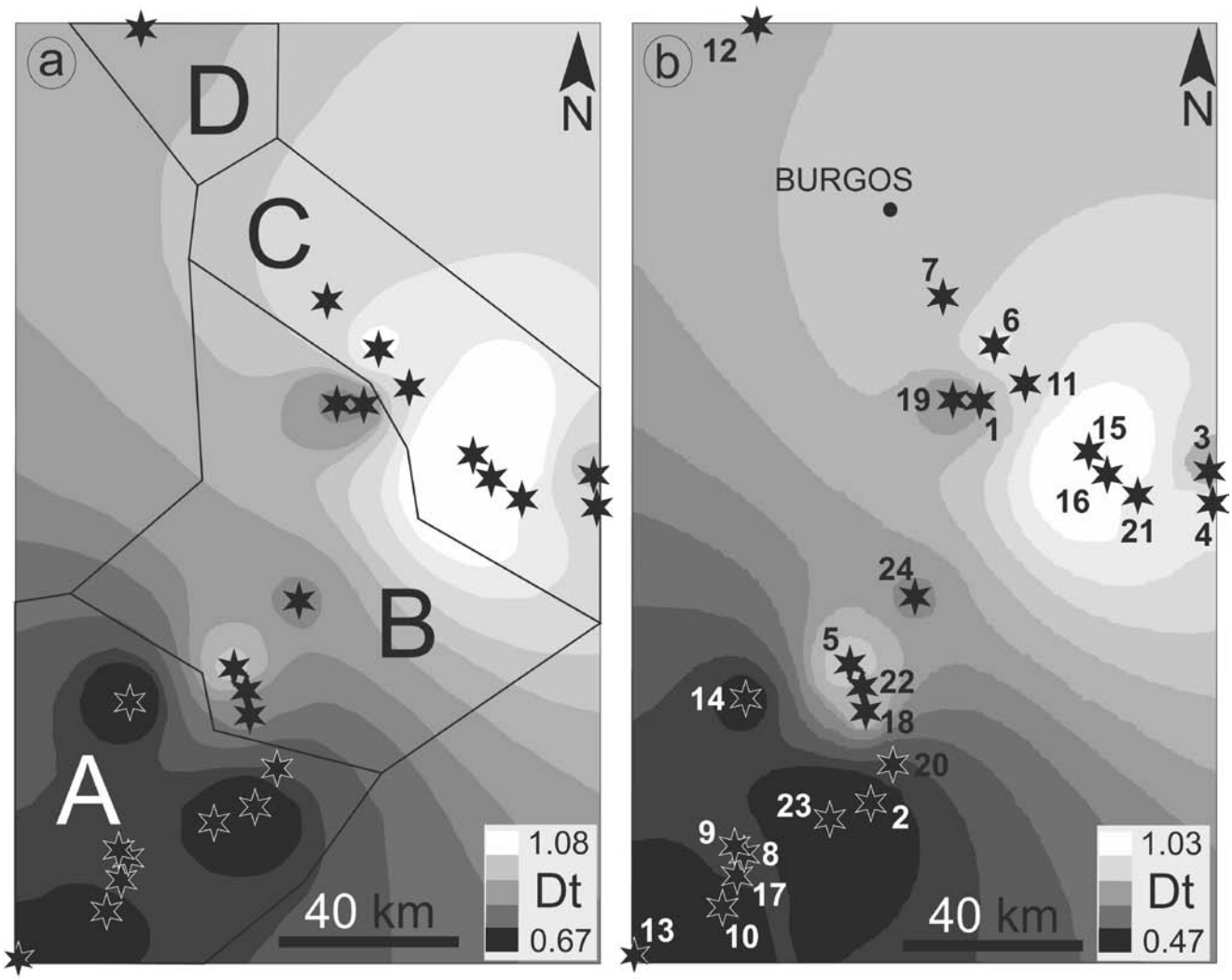

Fig. 6.- Uncorrected (a) and corrected (b) thickness distribution fractal dimension maps (D_t) of the studied area showing both the same pattern and relationships with sedimentary environments (b); A: coastal area; B: coastal and marine interdigitation area; C: shallow marine area; D: transition from shallow marine to distal platform environments. Stars and numbers refer to location of studied sections in Fig. 1 (see also Table 1).

distinct groups, whose main representatives are the Hoz de Silos, Arcones and Valdevacas and which are considered the end-members of all studied sections.

3) The multifractal spectra *f(α)* are generally symmetrical in shape and the amplitude *(Δα)* is used to discriminate the differences in the degree of homogeneity and consequently in the multifractality.
4) The Hoz de Silos section shows the lower amplitude value *(Δα* = 0.412) reflecting the lower degree of multifractality, which agrees with higher stratigraphical homogeneity (carbonate shelf environment). The Arcones section shows an intermediate amplitude value *(Δα* = 0.784) which corresponds to the coastal fringe, and the Valdevacas section shows the highest amplitude value *(Δα* = 1.123) reflecting the highest degree of heterogeneity and multifractality, which corresponds to the mixture of sedimentary processes that took place in relation to the coastal and shallow marine environments interdigitation.
5) The Hoz de Silos and Arcones sections show a more homogeneous behaviour within their sedimentary environments (either marine or coastal respectively) resulting in a decrease of the heterogeneity and multifractality.
6) Finally, there is a close relationship between the correlation dimension *(D_2)*, the fractal thickness distribution dimension *(D_t)* and sedimentary environments, which might be used to recognize depositional patterns and to predict and correlate sedimentological features of well-logs and stratigraphic sections.

Acknowledgements

This work was funded by Project PEII-2014-037-P of the Junta de Comunidades de Castilla–La Mancha and by the DGICYT Project CGL2009-03046/BTE-12008 (Ministerio de Ciencia e Innovación). The authors would like to thank Prof. Agustin Martin-Izard (Universidad de Oviedo) and an anonymous reviewer for their valuable suggestions and comments to improve the manuscript.

References

Agterberg, F.P., Cheng, Q., Brown, A. and Good, D. (1996a): Multifractal modelling of fractures in the Lac Du Bonnet batholith, Manitoba. *Computers & Geosciences*, 22: 497–507.

Agterberg, F.P., Cheng, Q. and Wright, D.F. (1996b): Fractal Modelling of Mineral Deposits. In: *Proceedings of the International Symposium on the Application of Computers and Operations Research in the Minerals Industries* (J. Elbrond and X. Tang, Eds), Montreal, 43–53.

Agterberg, F.P. (2007): New applications of the model of de Wijs in

regional geochemistry. *Mathematical Geology*, 39: 1–25.

Arias, M., Gumiel, P., Sanderson, D.J. and Martín-Izard, A (2011): A multifractal simulation model for the distribution of VMS deposits in the Spanish segment of the Iberian Pyrite Belt. *Computers & Geosciences*, 37: 1917-1927.

Bailey, R.J. and Smith, D.G. (2005): Quantitative evidence for the fractal nature of the stratigraphic record: results and implications. *Proceedings of the Geologists' Association*, 116: 129-138.

Burgess, P.M. (2008): The nature of shallow-water carbonate lithofacies thickness distributions. *Geology*, 36: 235–238.

Carlson, J. and Grotzinger, J.P. (2001): Submarine fan environment inferred from turbidite thickness distributions. *Sedimentology*, 48: 1331–1351.

Cheng, Q. (1994): Multifractal modelling and spatial analysis with GIS: gold potential estimation in the Mitchell-Sulphurets area, Northwestern British Columbia. PhD Thesis, University of Ottawa, 268 p.

Cheng, Q. and Agterberg, F.P. (1996): Multifractal modelling and spatial statistics. *Mathematical Geology*, 28: 1–16.

Dercourt, J., Gaetani, M., Vrielynck, B., Barrier, E., Biju-duval, B., Brunet, M.F., Cadet, J.P., Crasquin, S. and Sandulescu, M. (2000): *Atlas Peri-Tethys, Palaeogeographical Maps*. Commission for the Geologic Map of the World, Paris.

Drummond, C.N. and Wilkinson, B.H. (1996): Stratal thickness frequencies and the prevalence of orderedness in stratigraphic sections. *Journal of Geology*, 104: 1–18.

Evertsz, C.J.G. and Mandelbrot, B.B. (1992): Multifractal Measures (Appendix B). In: *Chaos and fractals: New Frontiers of Science* (H.-O. Peitgen, H, Jürgens, H, D. Saupe, Eds), Springer-Verlag, New York, 921–953.

Feder, J. (1988): *Fractals*. Plenum press, New York. 283 p.

Felletti, F. and Bersezio, R. (2010): Validation of Hurst statistics: a predictive tool to discriminate turbiditic sub-environments in a confined basin. *Petroleum Geoscience*, 16: 401-412.

Floquet, M., Alonso, A. and Meléndez, A. (1982): Cameros-Castilla. El Cretácico superior. In: *El Cretácico de España* (Á. García, Coord). Universidad Complutense. Madrid. 387–453.

Floquet, M., 1991. La plate-forme Nord-Castellane au Crétacé supérieur (Espagne). Ph. D. Thèse. Mémoires Géologiques de l'Université de Dijon 14, Dijon.

Gil, J., Segura, M. and García-Hidalgo, J.F. (2001): La Secuencia deposicional del Turoniense superior en el borde meridional de la Sierra de la Demanda (Cordillera Ibérica Septentrional; Provincias de Burgos y Soria). *Geotemas*, 3 (2): 205–208.

Gil, J., Carenas, B., Segura, M., García-Hidalgo, J.F. and García, A. (2004): Revisión y correlación de las unidades litoestratigráficas del Cretácico Superior en la región central y oriental de España. *Revista de la Sociedad Geológica de España*, 17 (3–4): 249–266.

Gil, J., García-Hidalgo, J.F., Segura, M., García, A. and Carenas, B. (2006a): Stratigraphic architecture, palaeogeography and sea-level changes of a third order depositional sequence: The late Turonian–early Coniacian in the northern Iberian Ranges and Central System (Spain). *Sedimentary Geology*, 191: 191–225.

Gil, J., Segura, M., García-Hidalgo, J. F. and Carenas, B. (2006b): High-frequency cyclicity in the Upper Cretaceous of the Northern Iberian Range (Spain). *Zeitschrift der Deutschen Gesellschaft für Geowissenschaften*, 157: 667–685.

Gil, J., García-Hidalgo, J.F., Mateos, R. and Segura, M. (2009): Orbital cycles in a Late Cretaceous shallow platform (Iberian Ranges, Spain), *Palaeogeography Palaeoclimatology Palaeoecology*, 274: 40–53.

Gomez, B.; Page, M., Bak, P. and Trustrum, N. (2002): Self-organized criticality in layered, lacustrine sediments formed by landsliding. *Geology*, 30: 519-522.

Grassberger, P. and Procaccia, I. (1983): Measuring the strangeness of strange attractors. *Physica D*, 9: 189-208.

Gumiel, P., Sanderson, D. J., Arias, M., Roberts, S. and Martín-Izard, A. (2010): Analysis of the fractal clustering of ore deposits in the Spanish Iberian Pyrite Belt. *Ore Geology Review*, 38: 307-318.

Kolmogorov, A.N. (1951): Solution of a problem in probability theory connected with the problem of the mechanism of stratification. *Transactions of the American Mathematical Society*, 53: 171–177.

Loehle, C. and Li, B. (1996): Statistical properties of ecological and geologic fractals. *Ecological Modelling*, 85: 271–284.

Longhitano, S.G. and Nemec, W. (2005): Statistical analysis of bed-thickness variation in a Tortonian succession of biocalcarenitic tidal dunes, Amantea Basin, Calabria, southern Italy. *Sedimentary Geology*, 179: 195–224.

Ludescher, J., Bogachev, M.I., Kantelhardt, J.W., Schumann, A.Y. and Bunde, A. (2011): On spurious and corrupted multifractality: The effects of additive noise, short-term memory and periodic trends. *Physica A*, 390: 2480–2490.

Mandelbrot, B.B. and Wallis, J.R. (1969): Global dependence in geophysical records. *Water Resources Research*, 5: 321-340.

Milenkovíc, B.S. (1989): Verification of the hypothesis regarding the random nature of fluctuation of geological properties. *Journal of Geology*, 97: 109–116.

Panahi, A. and Cheng, Q. (2004): Multifractality as a Measure of Spatial Distribution of Geochemical Patterns. *Mathematical Geology*, 36: 827-846.

Pettijohn, F.J. (1957): *Sedimentary Rocks*, Harper, New York, 2nd ed., 718 p.

Pickering, G., Bull, J.M. and Sanderson, D.J. (1995): Sampling power-law distributions. *Tectonophysics*, 248: 1-20.

Plotnick R.E. and Prestegaar, K.L. (1995): Fractal and Multifractal Models and Methods in Stratigraphy. In: *Fractals in Petroleum Geology and Earth Processes* (C.C. Barton and P.R. La Pointe, Eds). Plenum Press, New York. 73-98.

Reicherter, K.R. and Pletsch, T.K. (2000): Evidence for a synchronous circum-Iberian subsidence event and its relation to the African-Iberian plate convergence in the Late Cretaceous. *Terra Nova*, 12: 141-147.

Sadler, P.M. (1982): Bed-thickness and grain-size of turbidites. *Sedimentology*, 29: 37–51.

Schwarzacher, W. (1975): *Sedimentation Models and Quantitative Stratigraphy*. Elsevier, Amsterdam, 382 p.

Segura, M., Carenas, B., Gil, J., García-Hidalgo, J.F. and García, A. (2001): Anatomy of the carbonate bodies in relation to their position with respect to the maximum transgressive in the 2nd-order Cycles of the Upper Cretaceous from the Iberian Range. *Géologie Méditerranéenne*, 28: 163–168.

Segura, M., García, A., Carenas, B., García-Hidalgo, J.F. and Gil, J. (2002): Upper Cretaceous of the Iberian basin. In: *The Geology of Spain* (W. Gibbons and M.T. Moreno, Eds). The Geological Society of London. London. 288–292.

Sylvester, Z. (2007): Turbidite bed thickness distributions: methods and pitfalls of analysis and modeling. *Sedimentology*, 54: 847-870.

Talling, P.J. (2001): On the frequency distribution of turbidite thickness. *Sedimentology*, 48: 1297–1331.

Turcotte, D.L. (1992): *Fractals and Chaos in Geology and Geophysics*. Cambridge University Press. 221 p.

MANUSCRITO RECIBIDO EL 21-12-2015
RECIBIDA LA REVISIÓN EL 11-03-2016
ACEPTADO EL MANUSCRITO REVISADO EL 17-03-2016